

- (1977)]. Although it may be found in most terrestrial weathering environments, varnish is abundant in deserts where biogeochemical conditions are most favorable for genesis and preservation [R. I. Dorn and T. M. Oberlander, *Prog. Phys. Geogr.* 6, 317 (1982)].
3. R. I. Dorn, *Quant. Res. (N.Y.)* 20, 49 (1983).
  4. R. I. Dorn and M. J. DeNiro, *Science* 227, 1472 (1985).
  5. K. Kaegri and J. Iverson, *Textbook of Pollen Analysis* (Hafner, New York, ed. 3, 1975); O. P. Mehra and M. L. Jackson, *Clays Clay Miner.* 7, 317 (1958); T. T. Chao, *Soil Sci. Soc. Am. Proc.* 36, 764 (1972).
  6. A. J. T. Jull *et al.*, *Nucl. Instrum. Methods* 218, 509 (1983); D. J. Donahue *et al.*, *ibid.*, p. 425.
  7. R. I. Dorn and D. S. Whitley, *Ann. Assoc. Am. Geogr.* 74, 308 (1984).
  8. H. Shindo and P. M. Huang, *Soil Sci. Soc. Am. J.* 48, 927 (1984); C. J. Yapp and H. Poths, *Eos* 66, 423 (1985).
  9. T. A. Cahill, *Annu. Rev. Nucl. Part. Sci.* 30, 211 (1980); \_\_\_\_\_ *et al.*, *Nucl. Instrum. Methods* B3, 291 (1984).
  10. J. C. Dohrenwend *et al.*, *Geology* 12, 163 (1984).
  11. H. T. Ore and C. N. Warren, *Geol. Soc. Am. Bull.* 81, 2553 (1971); S. Wells *et al.*, in *Surficial Geology of the Eastern Mojave Desert, California*, J. C. Dohrenwend, Ed. (Geological Society of America, Reno, NV, 1984), p. 69.
  12. Recent research established that the fraction of airborne fallout containing particles smaller than 2  $\mu\text{m}$  is the basic source of varnish constituents (2, 3, 13). Scanning electron microscopy of historical, human-made surfaces in the Mojave Desert show no varnish growth after 50 to 70 years but the beginnings of varnish colonization in about 100 years (14). Thus 100 years B.P. is estimated to be the time required for the initiation of varnish growth and 100 years is assigned in Fig. 2 as the age of the <2- $\mu\text{m}$  fraction of aeolian deposits collected at the calibration and archeological sites (15).
  13. C. C. Allen, *J. Geol.* 86, 743 (1978); R. Perry and J. Adams, *Nature (London)* 276, 491 (1978); C. B. Moore and C. D. Elvidge, in *Handbook on the Deserts of North America*, G. L. Bender, Ed. (Greenwood, Westport, CT, 1982), p. 527.
  14. Incipient varnish was found on all exposures of faced rock surfaces at Fort Paiute (constructed in the eastern Mojave Desert in 1868). Seven energy-dispersive analyses of x-rays (EDAX) of the <2- $\mu\text{m}$  fraction of soil adjacent to Fort Paiute reveal a CR of  $8.7 \pm 0.1$ . Twenty-eight EDAX of varnish patches (seven from each side of Fort Paiute) yield a similar ratio of  $8.8 \pm 0.4$ , with four PIXE of the <2- $\mu\text{m}$  soil at  $8.80 \pm 0.50$ . Dorn and Whitley (7) also found that EDAX of surficial varnish layers in the Coso Range reflected accurately the  $\text{K}^+ + \text{Ca}^{2+} / \text{Ti}^{4+}$  ratio of adjacent soil material. These data indicate that the <2- $\mu\text{m}$  fraction of surficial soil material is a reasonable proxy for the  $\text{K}^+ + \text{Ca}^{2+} / \text{Ti}^{4+}$  ratio at the time of varnish initiation.
  15. The CR of surficial soil and dust in rock surface depressions from 20 sites scattered along the Mojave River sink averages  $8.56 \pm 0.36$ . Seven sites in the Cima volcanic field yield a CR of  $8.58 \pm 0.51$ . The CR for three sites at Silver Lake is  $8.58 \pm 0.87$ , and the CR averages  $8.55 \pm 0.33$  for the archeological sites.
  16. M. C. Rabenhorst, L. P. Wilding, C. L. Girdner, *Soil Sci. Soc. Am. J.* 48, 621 (1984); T. L. Péwé, E. A. Péwé, R. H. Péwé, A. Journax, R. M. Slatt, *Geol. Soc. Am. Spec. Pap.* 186, 169 (1981).
  17. M. E. Macko, E. B. Weil, D. B. Bamforth, *Intermountain Power Project Documentation for Determinations at Five Prehistoric Archaeological Sites Along the Intermountain-Adelanto Transmission Line 1 Right of Way, California Section* (Applied Conservation Technology, Fullerton, CA, 1983).
  18. We use 7000 to 4500 years B.P. as the approximate time period of the althermal for comparative purposes [C. M. Aikens, *Late-Quaternary Environments of the U.S.*, vol. 2, *The Holocene*, H. E. Wright, Ed. (Univ. of Minnesota Press, Minneapolis, 1983), p. 239].
  19. R. I. Dorn, in *Surficial Geology of the Eastern Mojave Desert, California*, J. C. Dohrenwend, Ed. (Geological Society of America, Reno, NV, 1984), p. 150.
  20. V. Haynes, *Science* 181, 305 (1973); R. E. Taylor and L. A. Payen, in *Adv. Archaeol. Method Theory* 2, 239 (1979); T. W. Stafford, Jr., *et al.*, *Nature (London)* 308, 446 (1984); J. L. Bada *et al.*, *ibid.* 312, 442 (1984); R. E. Taylor *et al.*, *Am. Anthropol.* 50, 136 (1985).
  21. R. D. Simpson, *Proc. Int. Congr. Am.* 35, 5 (1964); W. S. Glennan, *J. New World Archaeol.* 1, 43 (1976).
  22. W. S. Glennan, *Pac. Coast Archaeol. Soc. Quart.* 10, 17 (1974).
  23. R. M. Potter and G. R. Rossman [*Am. Mineral.* 64, 1219 (1979)] found romanechite or hollandite-group minerals called crack deposits in association with black rock varnish in the Mojave Desert.
  24. B. Curtiss, J. B. Adams, M. S. Ghiorso, *Geochim. Cosmochim. Acta* 49, 49 (1985).
  25. Funding for SBr-2100, -2162, -2223, and -3183 and most of the calibration was provided by the Los Angeles Department of Water and Power for the Intermountain Power Project. We thank R. Berger and D. M. McJunkin for assistance in evaluating the possible fractionation of varnish organic matter, D. Dorn for field assistance, H. Girey for artifact illustrations, M. Q. Sutton for noting historical sites, and anonymous reviews for comments.

15 March 1985; accepted 6 September 1985

## Periodic Extinction of Families and Genera

DAVID M. RAUP AND J. JOHN SEPKOSKI, JR.

Eight major episodes of biological extinction of marine families over the past 250 million years stand significantly above local background ( $P < 0.05$ ). These events are more pronounced when analyzed at the level of genus, and generic data exhibit additional apparent extinction events in the Aptian (Cretaceous) and Pliocene (Tertiary) Stages. Time-series analysis of these records strongly suggests a 26-million-year periodicity. This conclusion is robust even when adjusted for simultaneous testing of many trial periods. When the time series is limited to the four best-dated events (Cenomanian, Maestrichtian, upper Eocene, and middle Miocene), the hypothesis of randomness is also rejected for the 26-million-year period ( $P < 0.0002$ ).

SEVERAL INVESTIGATORS HAVE PROPOSED that major biological extinctions exhibit a stationary periodicity through geologic time (1-3), with estimated period lengths ranging from 26 to 32 million years. Each proposal has included the strong implication that the periodicity itself indicates a single driving mechanism, be it earthbound (1) or extraterrestrial (2, 3). We present new data and additional analyses to support our conclusion that extinctions during the last 250 million years follow a 26-million-year periodicity (2).

The claims of periodicity have produced considerable controversy (4). Many of the negative criticisms can be summarized by two fundamental arguments: first, periodicity is just an artifact of uncertainties in the geologic time scale or in the identification of

extinction events (5); second, periodicity is the natural consequence of many complex causes of extinction operating independently (5, 6).

The first argument says that inclusion of random noise in the form of spurious data could create the appearance of periodicity where none actually exists. The analyses in question (2, 3) start by asking whether extinction events are randomly distributed in time. This is the fundamental null hypothesis for formal statistical testing as well as the conventional wisdom in paleontology. Only if this hypothesis of randomness can be rejected with high confidence can a search for a nonrandom pattern begin. Inaccurate geologic dates or nonexistent extinction events will degrade the sample in a direction toward randomness and away

from any regular signal. Thus, to include uncertain data is to make statistical testing more conservative. To argue that uncertainty in the data explains the observed periodicity is illogical.

The second argument is based on a misconception of randomness. If extinction events (as opposed to individual species extinctions) are caused by a complex of time-independent processes, they should exhibit a random (Poisson) distribution in time, typified by irregular clusters of closely spaced events separated by gaps of widely varying length. Even if the individual events in a cluster cannot be distinguished because of poor time resolution, the clusters themselves will be irregularly spaced. The surprisingly uniform spacing of extinction events in Mesozoic-Cenozoic time is thus distinctly atypical of phenomena driven by complexes of independent processes.

Considerable confusion surrounds the definition of "mass extinction" and "extinction event." At one extreme, about five large events may be singled out as the mass extinctions and all others relegated to background. At the other extreme, a continuous range of extinction intensities may be treated, with the five largest events being analogous to the 100-year flood of hydrology and other,

Department of Geophysical Sciences, University of Chicago, Chicago, IL 60637.

smaller extinction events analogous to more frequent but less catastrophic floods. We have chosen the latter course on the grounds that a substantial number of time intervals have extinction levels significantly above those of adjacent intervals. Most of the extinction events identified in this way have long been recognized as times of high biological turnover and have been used since the mid-19th century to define the major units of geologic time.

The intensities of extinction events measured from the fossil record are subject to a great deal of measurement error and are influenced by choice of metric, sampling interval, and biostratigraphic time scale (2, 5). On the other hand, the positions of extinction peaks in time are generally far more stable. For this reason, our original analysis (2) worked only with the spacing of the 12 local maxima observed in the record from 253 to 11 million years ago. All extinction maxima were analyzed, regardless of magnitude. We have now tested each peak for statistical significance using calculated standard errors for the observed extinction intensities (7, 8).

Figure 1A illustrates the time series for all marine animal families (exclusive of those known only from Lagerstätten) in the 42 stratigraphic stages (including the Pleistocene near 0 million years) between 268 million years ago (mid-Permian) and the Recent. Approximately 2160 families, as opposed to the previous 567, are used. The error bars, computed assuming a Poisson model for the variance in extinction numbers per stage, permit assessment of the significance of maxima relative to local background (7, 8). At the 5 percent significance level, eight maxima appear statistically significant (that is, are 2 standard errors above neighboring minima): Guadalupian (or Dzhulfian), Norian (or Rhaetian), Pliensbachian, Tithonian, Cenomanian, Maestrichtian, upper Eocene, and middle Miocene (9). Each has been recognized independently as containing an extinction event on the basis of more detailed biostratigraphic evidence (8).

The eight maxima are also apparent in extinction time series for fossil genera, indicating that they are not simply artifacts of taxonomic level. Figure 1B illustrates a preliminary compilation of stratigraphic ranges

of marine animal genera (exclusive of vertebrates) (10). Forty-eight stratigraphic intervals (again including the Pleistocene) were used, with the five longest stages split into substages to make the sampling intervals more equal. Nearly 11,800 genera are represented, of which 9250 are extinct. Approximately 70 percent of these extinctions are resolved to the level of the stage or substage. The error bars are calculated to reflect counting error associated with high-resolution data and distributional error associated with low-resolution data (11).

Figure 1B shows that the extinction maxima for the smaller events are sharper and more clearly defined than at the familial level. This is particularly true for the upper Eocene and middle Miocene events. The generic data also contain a few maxima not evident among families: a Pliocene event, documented by Stanley and attributed to regional climatic change (12); a possible Aptian peak, predicted but not observed in the analysis of periodicity (8); and a Carnian maximum, which is probably an artifact of sampling (10).

Time-series analysis of the temporal distribution of extinction peaks is made difficult by the fact that the stratigraphic stages (bins) into which the data are compartmented are of highly uneven duration. This makes standard Fourier and autocorrelation techniques imprecise because they require interpolation of the data before analysis (13). Therefore, we have used the method developed by Stothers (14), in which the goodness of fit of the timings of the extinction events to a set of periodic impulse functions with differing wavelength is assessed. Goodness of fit is measured by the standard deviation of the differences between observed and expected times of extinction events for a given period length (in its best fit position). The lower the standard deviation, the better the fit. For each individual period length, the probability that the observed fit could have occurred by chance was computed by comparing that fit with fits obtained from a large number of randomized versions of the same data (15).

We have reanalyzed the time series in Fig. 1 using various combinations of the extinction events described above. Special attention was given to (i) the eight events determined to be significant in the familial data, (ii) the effect of including the new peaks indicated by the generic data (Aptian and Pliocene), and (iii) the portion of the time series including the four best-dated events.

Figure 2 shows goodness of fit for the eight significant familial extinction peaks for the past 268 million years, based on the ages given in (2): 248, 219, 194, 144, 91, 65,

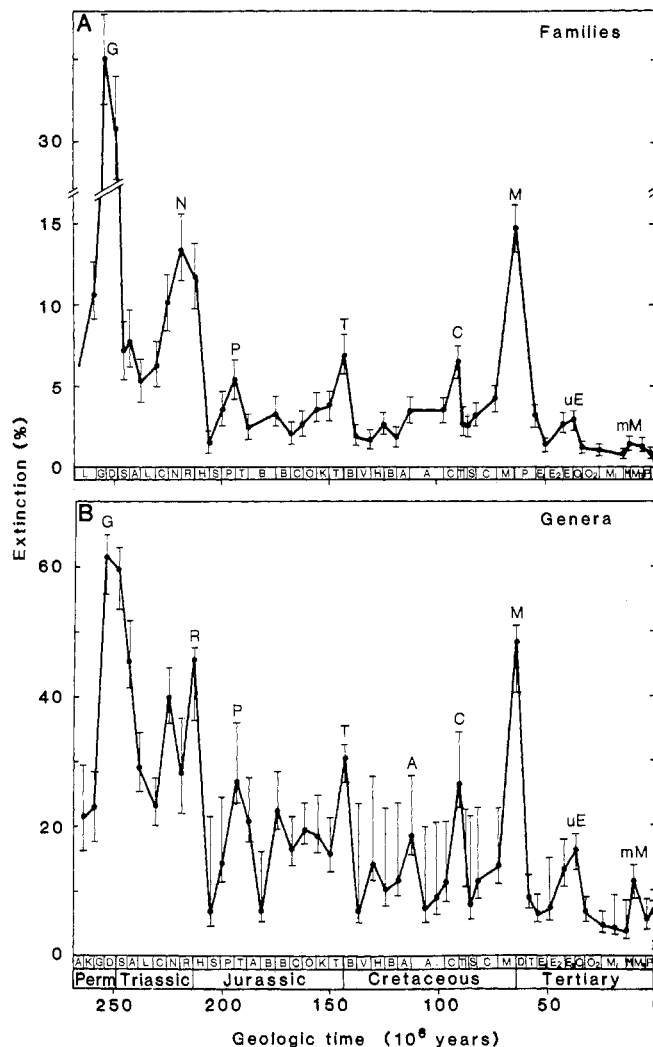


Fig. 1. Percentage of extinction for marine animal families (A) and genera (B) in stratigraphic intervals between the mid-Permian and the Recent. Letters along the abscissa denote standard stratigraphic units (17-19); letters above the time series show extinction events discussed. Error bars indicate one standard error of estimate (7, 11) above and below the observed values.

38, and 11.3 million years ago. The abscissa is plotted in the frequency domain rather than time domain. Note that goodness of fit increases downward on the ordinate. The heavy line shows the fit of the real time series over a frequency range of 0.016 to 0.080 per million years, corresponding to periods of 62.5 to 12.5 million years (the Nyquist limit). The real-time series shows sharp drops (improved fit) at frequencies of 0.038 and 0.077 per million years, representing periods of approximately 26 million years and its harmonic at 13 million years. The drop corresponding to 26 million years represents a statistically significant ( $P \ll 0.001$ ) rejection of the null hypothesis as judged by the confidence limits developed from randomization of the eight extinction events (solid curved lines in Fig. 2).

There is a nontrivial probability that any random time series will yield apparently significant results for some period, there being no a priori reason to focus on any single period. Because of this multiplicity of tests, we must ask what proportion of random time series with eight events cross the 99.9 percent curve (generated for each individual frequency) at any point in the frequency range. This was evaluated by tracking a new set of 500 random simulations, with each simulation monitored over the entire frequency range. Twenty-three of the simulations (4.6 percent) crossed the 99.9 percent curve, as indicated by the dots in Fig. 2. However, the fit of the real data at a frequency of 0.038 per million years is so strong that none of the simulations approached the real value, and we can thus be confident that this fit is not a chance result of multiple testing.

The analysis is complicated, however, by uncertainty about the placement of the Permian and Triassic events. In our earlier work, the Permian event was placed in the last stage (Dzulfian, ending 248 million years ago) and the Triassic event was placed in the penultimate stage (Norian, ending 219 million years ago) because the maxima in family extinctions were in these stages. Arguments can be made, however, for other choices. Both events are well known as major mass extinctions and are traditionally viewed as marking the Permo-Triassic and Triassic-Jurassic boundaries, respectively. But the paucity of continuous geologic sections makes their precise dating difficult. The Signor-Lipps effect is probably severe, causing a backward smearing of apparent extinctions due to artificial truncation of ranges (16). Therefore, we have analyzed the other three possible age combinations (253 and 219, 248 and 213, and 253 and 213 million years ago) in concert with the six well placed extinction events.

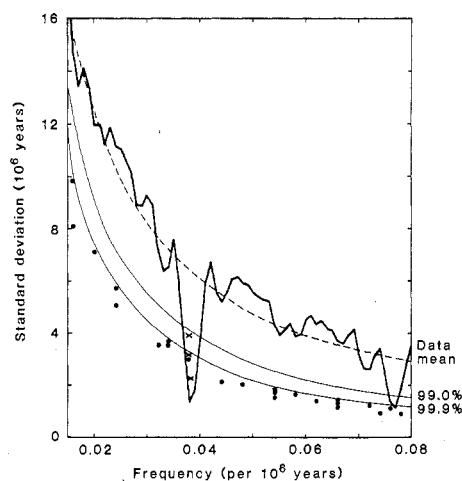


Fig. 2. Goodness of fit (standard deviation) of the eight statistically significant extinction events (the 248 and 219 million years ago combination of ages was used for the Permian and Triassic) over a range of frequencies (1/period). Goodness of fit increases downward. The excellent fit at a frequency of 0.038 per million years corresponds to the 26-million-year periodicity. The mean expectation (dashed curve) and 99.0 and 99.9 percent limits (solid curves) are based on randomized versions of the real-time series. Dots indicate the 23 of 500 independent randomizations that show better fits than the 99.9 percent limit. The x's at the 0.038 per million year frequency show goodness of fit when the other possible Permian and Triassic age combinations were used: Guadalupian-Norian (253 and 219 million years ago), Dzulfian-Rhaetian (248 and 213 million years ago), and Guadalupian-Rhaetian (253 and 213 million years ago).

The first case (253 and 219 million years ago) yields a goodness of fit (standard deviation) of 2.2 million years at a frequency of 0.038 per million years and is effectively no different from the case shown in Fig. 2. The second case (248 and 213 million years ago) has a goodness of fit value slightly below the 99.9 percent line; when multiple tests are evaluated, the significance level drops ( $P < 0.044$ ). The third case (253 and 213 million years ago) has a goodness of fit value of 3.9 million years for a frequency of 0.038 per million years which corresponds to a significance level of  $P < 0.007$ ; however, when multiple tests are evaluated, the overall significance level drops to a clearly nonsignificant value ( $P < 0.3$ ).

Thus, the choice of extinction points in the Permian and Triassic can strongly influence the confidence one has in a periodicity at 26 million years. Of the four ways in which the Permian and Triassic events can be placed, two show overwhelming rejection

of a random hypothesis ( $P < 0.01$ ), one allows rejection at the 5 percent significance level, and the other prevents rejection of the null hypothesis at an acceptable level.

The analyses were repeated with the addition of the Aptian and Pliocene extinction events suggested by the generic data, making a total of ten events. Dates of 248 and 213 million years ago were used for the Permian and Triassic, as a relatively conservative estimate of the actual times. The same strong improvement in fit was observed at the 0.038 per million year frequency, with  $P < 0.0015$  after 2000 random simulations. The earlier experience with the multiple test problem suggests at least a 5 percent significance level for the rejection of the null hypothesis. Even when the doubtful Carnian event is added, the fit is robust ( $P < 0.001$  with 2000 simulations).

Finally, the most recent four significant events, at 91, 65, 38, and 11.3 million years ago, were tested by the same procedure.

Table 1. Ages of extinction events with dates from three time scales (8).

System and stage	End of interval ( $\times 10^6$ years ago)			Event	
	Harland <i>et al.</i> (17)	DNAG (19)	Odin (18)	Families	Genera
Tertiary, Pliocene	2.0	1.6	1.9		Possible
Tertiary, middle Miocene	11.3	11.2	11	Significant	Present
Tertiary, late Eocene	38	36.6	34	Significant	Present
Cretaceous, Maestrichtian	65	66.4	65	Significant	Present
Cretaceous, Cenomanian	91	91	91	Significant	Present
Cretaceous, Aptian	113	113	107		Possible
Cretaceous, Hauterivian	125	124	114	Doubtful	
Jurassic, Tithonian	144	144	130	Significant	Present
Jurassic, Callovian	163	163	150	Doubtful	
Jurassic, Bajocian	175	176	170	Doubtful	
Jurassic, Pliensbachian	194	193	189	Significant	Present
Triassic					
"Rhaetian"	213	208	204		Present
Norian	219	216	209	Significant	
Triassic, Carnian	225	225	220		Doubtful
Triassic, Olenekian	243	240	239	Doubtful	
Permian					
Dzulfian	248	245	245	Significant	
Guadalupian	253	253	252	Significant	Present

This is an especially important case because the events of the last 100 million years are the most accurately dated and because the several available geologic time scales (17–19) are nearly identical for this interval (Table 1). The goodness of fit at the 0.038 per million years frequency is a striking 0.46 million years, which is stronger than all but one of 5000 random simulations run for the four-event case ( $P < 0.0002$ ).

We conclude that the claim for a stationary periodicity with a spacing of approximately 26 million years is strong enough to merit further search for confirming evidence. Because we are dealing with statistical inference in a complex situation, completely satisfactory conclusions will be reached only with higher resolution data on extinction and on other relevant aspects of biological and geological history.

#### REFERENCES AND NOTES

1. A. G. Fischer and M. A. Arthur, *Soc. Econ. Paleontol. Mineral. Spec. Publ.* 25 (1977), p. 19.
2. D. M. Raup and J. J. Sepkoski, Jr., *Proc. Natl. Acad. Sci. U.S.A.* 81, 801 (1984).
3. M. R. Rampino and R. B. Stothers, *Nature (London)* 308, 709 (1984); *Science* 226, 1427 (1984).

4. See A. Hallam, *Nature (London)* 308, 686 (1984); R. A. Kerr, *Science* 227, 1451 (1985); J. Maddox, *Nature (London)* 315, 627 (1985).
5. A. Hoffman and J. Ghiold, *Geol. Mag.* 122, 1 (1984); A. Hoffman, *Nature (London)* 315, 659 (1985).
6. G. B. Wilson, *Nature (London)* 315, 272 (1985).
7. For percent of familial extinction, 1 standard error on either side of the observed value can be estimated approximately as  $[(E_i/D_i)^{1/2} \pm (1/(4D_i))^{1/2}]^2$ , where  $E_i$  is the number of extinctions in the  $i$ th stage and  $D_i$  is the standing diversity (assumed to be without error). See Sepkoski and Raup (8) for details.
8. J. J. Sepkoski, Jr., and D. M. Raup, in *Dynamics of Extinction*, D. Elliott, Ed. (Wiley, Somerset, NJ, 1986), pp. 3–36.
9. We note that these eight maxima are separated by an average of approximately five stages, which may be the source of J. A. Kitchell and D. Pena's [*Science* 226, 689 (1984)] calculated "pseudoperiodicity" of 31 million years (= 5 stages  $\times$  6.2 million year average duration per stage).
10. J. J. Sepkoski, Jr., in *Pattern and Process in the History of Life*, D. Jablonski and D. M. Raup, Eds. (Springer, Berlin, in press).
11. For generic data, error bars are computed as follows: for high-resolution data, standard errors of estimate were computed as in (7); for low-resolution data, assumed 99 percent confidence limits were computed as the difference between a given stage containing all distributed data and no distributed data. The error bar on each side of the observed percentage of generic extinction was thus estimated as the value for the high-resolution data plus one-third the value of low-resolution data.
12. S. M. Stanley, *Macroevolution: Pattern and Process* (Freeman, San Francisco, 1979); ———, in *Extinctions*, M. H. Nitecki, Ed. (Univ. of Chicago Press, Chicago, 1984), p. 69; *Geology* 12, 205 (1984); ——— and L. D. Campbell, *Nature (London)* 293, 457 (1981).
13. Standard methods of time-series analysis that would fit regular functions to the extinction data are of dubious value also because there is no reason to assume any pattern in the magnitudes (as opposed to timing) of the events and because extinction intensities during events may not be continuous with background intensities.
14. R. B. Stothers, *Astron. Astrophys.* 77, 121 (1979). Stothers assumed that, given the event times  $t_i$ , for  $i = 1, \dots, n$ , they can be modeled by the equation  $t_i = t_0 + j_i P + e_i$ , where  $P$  is the period,  $t_0$  is the phase, and  $j_i$  is the integer value that minimizes the square of  $e_i = t_i - t_0 - j_i P$ , where  $e_i$  is the error term. Values of  $[\sum_{i=1}^n e_i^2 / (n - 1)]^{1/2}$  are plotted in Fig. 2.
15. We empirically generated the distribution of the error term (14) for each frequency ( $1/P$ ) by randomly locating the  $n$  events among the geologic stages. However, because the actual data cannot reveal extinction events in contiguous stages, randomizations were constrained so that only one event could fall in any given stage, and adjacent events were separated by at least one stage without an event.
16. P. H. Signor III and J. H. Lipps, in *Geological Implications of Impacts of Large Asteroids and Comets on the Earth*, L. T. Silver and P. H. Silver, Eds. (Geological Society of America, Boulder, CO, 1982), p. 291.
17. W. B. Harland, A. V. Cox, P. G. Llewellyn, C. A. G. Picton, A. G. Smith, R. Walters, *Geologic Time Scale* (Cambridge Univ. Press, Cambridge, England, 1980).
18. G. S. Odin, Ed. *Numerical Dating in Stratigraphy* (Wiley, Somerset, NJ, 1982).
19. For "DNAG" time scale, see A. R. Palmer, *Geology* 11, 503 (1983).
20. Supported by NASA grants NAG-237 and NAG-282. We thank A. Hallam, D. Jablonski, S. M. Stigler, S. Tremaine, and three anonymous reviewers for helpful discussions and criticism.

5 August 1985; accepted 10 December 1985

## Thermal Spectrum of Uranus: Implications for Large Helium Abundance

GLENN S. ORTON

An analysis of the infrared spectrum of Uranus' disk between 7 micrometers and 3 millimeters suggests a volume mixing ratio for helium in the atmosphere of  $40 \pm 20$  percent, more than for the sun, Jupiter, or Saturn. Alternative explanations require even more extreme assumptions regarding gas abundances or aerosol vertical distribution and spectral properties. The most serious difficulty with a model containing large amounts of helium is devising a credible evolutionary or chemical model explaining the absence or segregation of so much hydrogen.

MANY OF THE RECENT EARTH-based observations of the thermal spectrum of Uranus between 7  $\mu$ m and 3 mm (1–5) were inspired by the need to support the upcoming Voyager 2 investigation of the atmosphere by providing observations of the spectrum where the spacecraft infrared experiment (IRIS) is not sensitive. I undertook an examination of these data to derive a provisional model for the disk-averaged temperature and composition and to evaluate the influence of clouds on the outgoing thermal radiance spectrum. The results of the analysis were surprising because they imply a bulk gas composition very unlike those of Jupiter or Saturn.

*Data.* All the data used in this study are

shown in Fig. 1. No data were used with observational uncertainty greater than 3.5 K, and data were generally excluded whose spectral resolution ( $\lambda/\Delta\lambda$ ) was less than 1.7; some nearly coincident observations (2, 3) were averaged together. The newest data in the 400- to 1400- $\text{cm}^{-1}$  range (5) are consistent with earlier filtered radiometry (6, 7) in the same spectral region. The outline of  $\text{H}_2$  collision-induced absorption is apparent with a broad translational band near 100  $\text{cm}^{-1}$  and strong rotational lines,  $S(0)$  and  $S(1)$ , located, respectively, near 365 and 600  $\text{cm}^{-1}$ ; double transitions are also located near 950 and 1200  $\text{cm}^{-1}$ . As appropriate, data were recalibrated in the following ways. A 1-bar equatorial radius of 25,563 km was

adopted uniformly (2–4). The observations, with Mars used for absolute calibration (2–4), were revised through an improved thermophysical model to predict the outgoing thermal radiance of that planet (8). The calibration of other observations was modified, consistent with a recent revision of the infrared stellar flux scale (9). The effect of the recalibrations is to bring different data sets into closer agreement with each other, although the major conclusions of this research would be unchanged without the recalibration. However, it does decrease the bolometric thermal output to be equivalent to an effective temperature of  $57.7 \pm 2.0$  K as compared to an earlier estimate of  $58.3 \pm 2.0$  K (3).

*Model procedure.* Recovery of the temperature was possible between about 40 mbar and 8 bars total pressure. The opacity of  $\text{H}_2$  induced by collisions with  $\text{H}_2$ , He, and  $\text{CH}_4$  was modeled by ab initio calculations that should be accurate in the relevant temperature range (about 50 to 150 K) within 5 percent throughout most of the spectrum and 15 percent at high frequencies, with relative accuracy much better than these values (10). The influence of discrete dimer

Earth and Space Sciences Division, Jet Propulsion Laboratory, California Institute of Technology, Pasadena 9109.